ISSN: 1410-8917
e-ISSN: 2597-9914

Jurnal Kimia Sains dan Aplikasi 23 (3) (2020): 68–74

Jurnal Kimia Sains dan Aplikasi
Journal of Scientific and Applied Chemistry

Journal homepage: http://ejournal.undip.ac.id/index.php/ksa

Synthesis and Characterization of Triamine modified coated Iron Sand Hybrid Nanomaterials originating from Kendal Coast

Ricka Prasdiantika [a,1], Susanto Susanto [b,2,*], Yustika Kusumawardani [a,3]

[a] Faculty of Engineering, Pandanaran University, Semarang 50268, Indonesia
[b] Department of Chemical Engineering, State Polytechnic of Malang, Malang 65141, Indonesia.

* Author email: (1) ricka.prasdiantika@unpand.ac.id, (2,*) susanto.s@polinema.ac.id, (3) yustika@unpand.ac.id

https://doi.org/10.14710/jksa.23.3.68-74

Article Info

Article history:

Received: 2nd September 2019
Revised: 10th February 2020
Accepted: 11th March 2020
Online: 31st March 2020

Keywords:
synthesis; nanomaterial; iron sand; Kendal; propyl diethylenetriamine

Abstract

Nanomaterials have broad and unique applications in various fields. In this research, synthesis of Iron Sand Magnetic Hybrid nanomaterials coated with propyldiethylenetriammine modified silica (PB@SiO_2@TA) originating from the coast of Muara Kencan, Kendal Regency. This study began with iron sand preparation, continued with activation, dispersing iron sand, then coating iron sand with propyldiethylenetriammine modified silica. The resulting product was characterized by X-Ray Fluorescence (XRF), Fourier Transform Infrared (FT-IR) Spectrophotometer, X-Ray Diffractometer (XRD), and Transmission Electron Microscope (TEM). The characterization results show that the iron sand of the coast of Muara Kencan Beach has a high iron oxide content (81.66%) with minerals in the form of magnetite. The characterization results also showed that the nanomaterial hybrid iron sand coated with propyldiethylenetriammine modified silica (PB@SiO_2@TA) was successfully synthesized with a crystal size of 36.21 nm, with better particle dispersion than the prepared iron sand.

1. Introduction

Nanomaterials have broad applications in various fields such as health, material coating, adsorption, sensors, and catalysts [1, 2, 3, 4, 5, 6]. Nanomaterials have a large surface area, high reactivity, large adsorption capacity, and fast adsorption rate [7]. Nanomaterial in the form of magnetite (Fe_3O_4) can be used in the process of adsorption of heavy metals because Fe_3O_4 facilitates the process of separating the adsorbent from the solution in the Batch system through the use of external magnets [8]. Fe_3O_4 in nature is found in iron sand, where natural iron sand also has other iron oxide compositions in the form of hematite (α-Fe_2O_3) and maghemite (γ- Fe_2O_3) [9]. Iron sand is abundant on the coast of Central Java Province, one of which is in the Kendal Regency [10]. However, magnetite tends to form aggregates, so dispersing agents such as sodium citrate is needed [11].

Inorganic-organic hybrid material has potential as an adsorbent. Silica gel is used as an inorganic matrix on inorganic-organic hybrid materials that are stable under acidic conditions, inert to redox reactions, and can be modified with functional groups, thereby increasing adsorbent selectivity [12, 13, 14]. The method used to coat silica on a magnetic material is the Stöber method through the sol-gel process [15]. Where the silica gel precursor that is more often used is sodium silicate because of its low price and low toxicity [16], the surface of silica can be modified with active clusters of organic compounds such as the mercapto group (-SH) or amine group ($-NH_2$) to increase selectivity in adsorbing heavy metal ions. Diamine grouped adsorbents can adsorb heavy metals better than mercapto group adsorbents [17].

In order to improve the ability to adsorb heavy metals, an organic compound with three amine groups of N^1-(3-trimethoxysilpropyl) diethylenetriamine (TMSPDETA) was used to modify silica-coated iron sand. The pH factor influences the type of interaction that occurs between the metal and the adsorbent surface. At low pH (pH <4.9), the protonated amine group ($-NH_2$) forms $-NH^{3+}$ as Lewis acid so that it can bind to a metal anion complex [18]. However, at pH> 4.9, the $-NH_2$ group tends to be a Lewis base so that it can bind metal cations

[18]. Thus, it is expected that the magnetized silica hybrid nanomaterial modified triamine group can be utilized as an adsorbent in further research. The purpose of this study was to synthesize and characterize the triamine modified silica-coated iron sand hybrid material (PB@SiO_2@TA). The benefit of this research is the production of a hybrid triamine modified silica-coated iron sand material (PB@SiO_2@TA).

2. Methodology

The stages of this research consisted of a) Preparation of iron sand magnetic material treated with water and characterization of the preparation material. b) Coating of iron sand material by adding Na_2SiO_3 and TMSPDETA solution and continued with a characterization of the synthesized material.

2.1. Equipment and Materials

The equipment for preparation consists of a measuring cup, beaker glass, volumetric flask, porcelain mortar, sonicators, ovens, analytical balance, external magnets (Niobium), and shakers. While the analysis equipment consists of X-Ray Fluorescence (PAnalytical Minipal 4) for identification of the constituent elements of materials, Fourier Transform Infrared Spectrophotometer (FT-IR, Shimadzu Prestige 21) for identification of functional groups of materials, X-Ray Diffractometer (XRD, XRD-6000 Shimadzu) for identification of mineral types, material size and crystallinity, and Transmission Electron Microscope (TEM, JEOL TEM-1400) for observing the morphology and dispersion of materials.

The material used consisted of iron sand from Muara Kencan Beach, Kendal Regency, Central Java, 37% HCl (Merck), Sodium Citrate (Aldrich), Na_2SiO_3 with SiO content of 25.5-28.5%, N-(3-trimethoxysilylpropyl) diethylenetriamine (TMSPDETA) 99% (Aldrich), and universal pH paper.

2.2. Iron Sand Magnetic Material Preparation

The essential ingredients of iron sand were separated using an external magnet. Solids attracted by external magnets were dried in an oven at a temperature of 70-80°C for 24 hours, then crushed and weighed. The obtained iron sand powder was characterized by XRF, FT-IR spectrophotometer, XRD, and TEM.

2.3. Activation and Dispersion of Iron Sand Magnetic Materials

Five grams of magnetic iron sand from the preparation was then put into a beaker. Then washed with distilled water and sonicated for 30 minutes and repeated three times. After that, the magnetic material in the beaker was washed using a 10 mL HCl solution and sonicated for 30 minutes, then rinsed using distilled water to neutral pH. An external magnet separated the mixture obtained in the beaker, and the sediment is taken. The activated magnetic material was then added with 100 mL of 0.5 M sodium citrate solution and allowed to stand for 24 hours. The obtained solid was separated with an external magnet and dried in an oven at a temperature of 70-80°C for 24 hours. Then the solid was crushed, weighed, and characterized with XRF, FT-IR spectrophotometer, XRD, and TEM.

2.4. Coating of iron sand magnetic material by triamine modified silica

The process of coating iron sand material by silica gel and the attachment of a group of propyldiethylenetriammine to the surface of silica was conducted through the sol-gel process. Three grams of iron sand material were acidified with 1 mL 1 M HCl solution, and the precipitate was taken (Mixture 1). Then as much as 3.0 mL of Na_2SiO_3 solution added with 1.2 mL of distilled water and 1.8 mL of TMSPDETA, then sonicated for 30 minutes (Mix 2). Then mixture 2 was put into a container containing mixture 1 and sonicated for 10 minutes. After that into the mixture, 1 M of HCl solution was added dropwise to pH of 7, and a gel was formed. Then, the gel formed was sonicated for 30 minutes and left for 24 hours. After aging, the gel was washed with distilled water to a neutral pH, separated with an external magnet, and the sediment was taken. The precipitate obtained was dried in an oven at 80°C for 24 hours. After drying, the solid was crushed and separated using an external magnet. Solids attracted by magnets were weighed and characterized by FT-IR, XRD, and TEM spectrophotometers.

2.5. Data analysis

Data analysis of iron sand material coating by silica gel and clustering was performed by interpreting the data obtained from the results of the characterization of the synthesized material.

Iron Sand Material Content. XRF analysis was used to identify the magnetic material content of the iron sand in Muara Kencan Beach, Kendal Regency, Central Java.

Functional Group. FT-IR spectrophotometer analysis is used to qualitatively identify the presence of functional groups contained in a sample compound.

Crystallinity and particle size. The XRD analysis method is used to obtain X-ray diffraction patterns. The characteristic peak diffraction angle of magnetite is at 2θ=30.0°; 35.4°; 43.0°; 53.4°; 56.9°; and 62.5° with Miller's index values of 220, 311, 400, 422, 511 and 440, respectively [19]. Through XRD data, crystal size can be determined using the Debye-Scherrer equation [20]:

$$D = \frac{0{,}9\,.\,\lambda}{\beta \cos\theta}$$

where D = Crystal size (nm), λ = wavelength of the metal atom used (nm), β = half the width of the peak FWHM (radians), θ = Bragg diffraction angle (degrees). The crystallinity of the magnetic material can be seen from the intensity of the X-ray diffraction peak. A sharper peak in XRD indicates higher crystallinity [21]. Based on the XRD pattern, magnetite coated with silica has lower crystallinity compared to magnetite coated with citrate, due to the amorphous nature of silica [22]. Amorphous silica has a characteristic peak at 2θ = 20-26° [23].

Morphology. TEM is used to determine the dispersion of magnetite nanomaterials [11] and see the

image of the coated material. The magnetite part is black, while the silica layer is gray [15].

Table 1. FT-IR wave numbers of sodium citrate dispersed magnetite nanomaterials and amine-modified Fe_3O_4@SiO_2

wavenumber (cm^{-1})	Identification	reference
466	Si-O-Fe stretching vibrations	[24]
540	vibrational stretches of Fe-O bonds	[25]
805	Si-O-Si symmetry stretching vibrations	[22]
1092	Si-O-Si asymmetry stretching vibrations	[24]
1307-1463	–COO– symmetry stretching vibrations	[11]
1458-1645	N-H bending vibration	[26]
1628–1636, 3441–3487	–OH vibration stretching groups of Fe-OH and Si-OH	[11, 16]
2900	C-H asymmetrical stretching vibrations	[8]
2850	C-H symmetry stretching vibrations	[8]

3. Results and Discussion

Iron sand samples were obtained from the Muara Kencan Beach, Kendal Regency, Central Java Province. Iron sand was prepared using an external magnet to separate the material content of the iron sand from its impurities; then, it is washed with distilled water, then dried. Then the iron sand was activated using 1 M HCl solution and 0.5 M sodium citrate solution. The iron sand magnetic material obtained had a black color, which indicated that the iron sand was dominated by the magnetic iron oxide content (Fe_3O_4). This result was following the characteristics of magnetite proposed by Cornell and Schwertmann [9].

Magnetic material for iron sand preparation, activated iron sand material, and the synthesized product in the form of hybrid triamine modified silica-coated iron sand material (PB@SiO_2@TA) were characterized to find out the success of synthesis with a) analysis of material contained in iron sand with X-Ray Fluorescence (XRF), b) functional group analysis with Fourier Transform Infrared (FT-IR) Spectrophotometer for analysis of functional groups in materials, c) analysis of crystallinity and crystal size with X-Ray Diffractometer (XRD) for analysis, and morphological analysis with Transmission Electron Microscope (TEM).

1.1. Results of analysis of material contained in iron sand (XRF test)

The results of XRF characterization on iron sand from the preparation and activation results are shown in Table 2. Based on Table 2, it is known that the magnetic material of the iron sand coast of Muara Kencan Beach has a content that is dominated by iron (Fe) and a minority content of impurities such as Ti, Si, Al, Ca, V, Mn, Eu, Rb, Re, K, P, Cr, and Zn. Meanwhile, activated iron sand showed an increase in iron content compared to prepared iron sand, from 81.66% to 82.64%. This is because some of the impurities have dissolved in the HCl acid solution used in the activation process.

Table 2. Results of XRF characterization in prepared and activated iron sands

Elements	Composition (%)	
	Prepared iron sand	Activated iron sand
Fe	81.66	82.64
Ti	6.75	6.80
Si	4.1	2.6
Al	2.3	3
Ca	1.21	0.96
V	0.64	0.64
Mn	0.62	0.56
Eu	0.54	0.36
Rb	0.41	0.29
Re	0.3	0.59
K	0.24	0.08
P	0.2	0.19
Cr	0.16	0.16
Zn	0.09	0.08

3.1. Iron Sand and PB@SiO_2@TA functional groups

The results of FTIR characterization on magnetic iron sand were prepared, activated iron sand, citric acid dispersed iron sand, and the PB@SiO_2@TA were shown in Figure 1

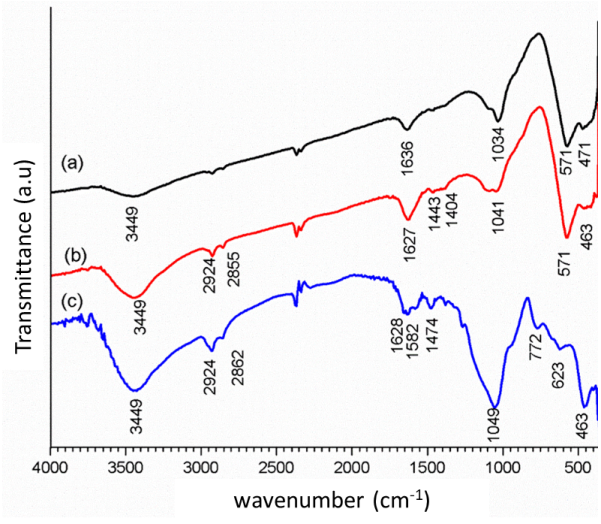

Figure 1. FTIR spectra of synthesized material: a) preparation sand iron, b) citric dispersed activated iron sand, and c) PB@SiO_2@TA

From Figure 1, the prepared iron sand has the peaks of FTIR spectra at 471, 571, 1034, 1636, and 3449 cm^{-1}. Activated iron sand has peaks of FTIR spectra at 463, 571, 1041, 1404, 1443, 1627, 2855, 2924, and 3449 cm^{-1}. Meanwhile, hybrid triamine modified silica-coated iron

sand material has FTIR spectra peaks at 463, 623, 772, 1049, 1474, 1582, 1627, 2862, 2924, and 3349 cm^{-1}.

Based on Figure 1 and Table 1, wave numbers at 463 cm^{-1} and 471 cm^{-1} indicate the existence of Si-O-Fe stretching vibrations. Wave numbers at 571 cm^{-1} and 623 cm^{-1} indicate the existence of stretching vibrations of the Fe-O bond of magnetite. The wavenumber at 772 cm^{-1} indicates the symmetric stretching vibration of Si-O-Si from propyldiethylenetriammine modified silica groups. Wave numbers at 1034-1049 cm^{-1} indicate the existence of Si-O-Si asymmetric stretching vibrations. Wave numbers at 1404 cm^{-1} and 1443 cm^{-1} indicate the presence of symmetric stretching vibrations –COO– of the citrate group. Wave numbers at 1474 cm^{-1} and 1582 cm^{-1} indicate the presence of N-H buckling vibrations from the propyldiethylenetriammine group. Wave numbers at 1627-1636 cm^{-1} and 3449 cm^{-1} indicate the existence of stretching vibrations of the -OH group from Fe-OH and Si-OH. Wave numbers at 2855-2866 cm^{-1} and 2924 cm^{-1} indicate symmetry stretching vibrations and C-H asymmetries.

Based on Figure 1 shows that the prepared and activated iron sands and PB@SiO_2@TA have a -OH functional group and a Fe-OH bond that shows the iron oxide content of magnetic material. The prepared and activated iron sands also still have impurities in the form of silica. The iron sand activated by HCl and sodium citrate also has a –COO– group and a C–H bond from the citrate group that demonstrates that the citric dispersed activated iron sand was successfully synthesized. In PB@SiO_2@TA, there is also a Si-O-Si bond with symmetric stretching vibrations, N-H and C–H bonds of the propyldiethylenetriammine group, the -OH group from Si-OH which shows that the activated iron sand was successfully coated with a propyldiethylenetriammine modified silica group. Thus, PB@SiO_2@TA was synthesized successfully.

3.2. Crystallinity and size of iron sand mineral and PB@SiO_2@TA

The results of XRD characterization on the prepared iron sand magnetic material, citric dispersed activated iron sand, and PB@SiO_2@TA are shown in Figure 2. Identification of the type of oxide minerals was carried out by matching the Fe_3O_4 diffraction pattern standard of JCPDS 00-001-1111 with six diffraction peaks are characteristic of magnetite with the Miller index of 220°, 311°, 400°, 422°, 511°, and 440°.

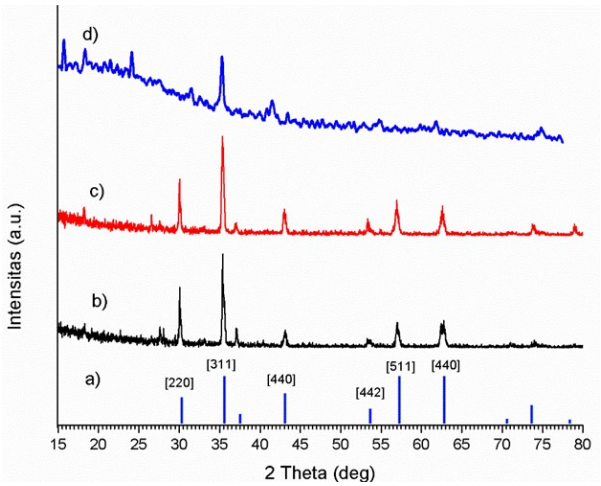

Figure 2. XRD diffractogram of a) JCPDS magnetite 01-1111, b) prepared iron sand, c) citric dispersed activated iron sand, and d) PB@SiO_2@TA

Based on Figure 2, the XRD diffraction pattern on the prepared iron sand material, citric dispersed-activated iron sand, and PB@SiO_2@TA match with peaks of 2θ on the standard Fe_3O_4 diffraction pattern of JCPDS 00-001-1111. This indicates that all these materials contain minerals containing iron oxide magnetite (Fe_3O_4).

Table 3. Comparison of crystal size and intensity of diffraction patterns in prepared iron sand, citric dispersed-activated iron sand, and PB@SiO_2@TA

Material	Size (D_{xrd}, nm)	the intensity of diffraction patterns
prepared iron sand	41.93	314
citric dispersed-activated iron sand	33.78	325
PB@SiO_2@TA	36.21	300

The crystallite size of the prepared iron sand, activated iron sand, and PB@SiO_2@TA are determined by the Debye-Scherrer equation, as suggested by Wu *et al.* [20]. Meanwhile, crystallinity is determined based on the intensity of the diffraction pattern, as stated by Hui *et al.* [21]. Determination of crystal size and intensity of diffraction pattern peaks at Miller index: 220, 311, 400, 422, 511, and 440 for the prepared iron sand material, citric dispersed-activated iron sand, and PB@SiO_2@TA are shown in Table 3.

Based on Table 3, the sizes of iron sand crystals are prepared, citric dispersed-activated iron sand, and PB@SiO_2@TA has nanoparticle size because it has a size in the range 1-100 nm referring to Kamal [2]. Activated iron sand has a smaller crystal size and a higher diffraction pattern intensity than the prepared sand iron. This may be since the prepared iron sand is only washed with distilled water, so the particles are still in the form of aggregates and have lower crystallinity because they still have more amorphous silica impurities, as suggested by Prasdiantika and Susanto [27]. Whereas in activated iron sand material, which is iron sand washed with HCl solution, impurities are lost and soaking with sodium citrate solution reduced aggregation of magnetite

particles as suggested by [19, 28, 29] and supported the TEM results in Figure 3.

PB@SiO_2@TA material has a larger crystal size and lower intensity of diffraction pattern compared to activated iron sand. This is due to the effect of amorphous modified silica propyldiethylenetriammine groups on PB@SiO_2@TA material, as indicated by a diffraction pattern that is inflated, as stated by Hong *et al.* [22] and Tan *et al.* [23]. This shows that the activated iron sand was successfully coated with a propyldiethylenetriammine modified silica. Thus PB@SiO_2@TA was synthesized successfully.

3.3. Morphology of PB@SiO_2@TA

The images of Transmission Electron Microscopy (TEM) on prepared iron sand and citric dispersed activated iron sand with a magnification of 500 nm are shown in Figure 3.

The TEM image in Figure 3 shows that the iron sand produced from activated citrate dispersed (3b) has a more evenly dispersed particle dispersion than the prepared iron sand (3a). That is because sodium citrate in activated iron sand has succeeded in reducing the aggregation of magnetite material in iron sand. The black color in the TEM (3a) image of the prepared iron sand is a magnetite particle, while the gray part is a silica impurity element, as stated by Li *et al.* [15]. While the gray color in the TEM (3b) image of activated iron sand dispersed by citrate groups is a citrate layer with impurities in the form of silica.

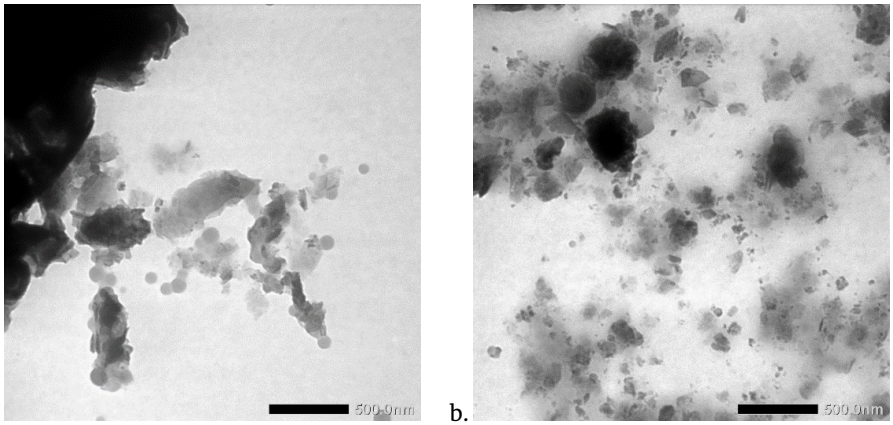

Figure 3. The images of Transmission Electron Microscopy (TEM) on (a) prepared iron sand and (b) citric dispersed-activated iron sand

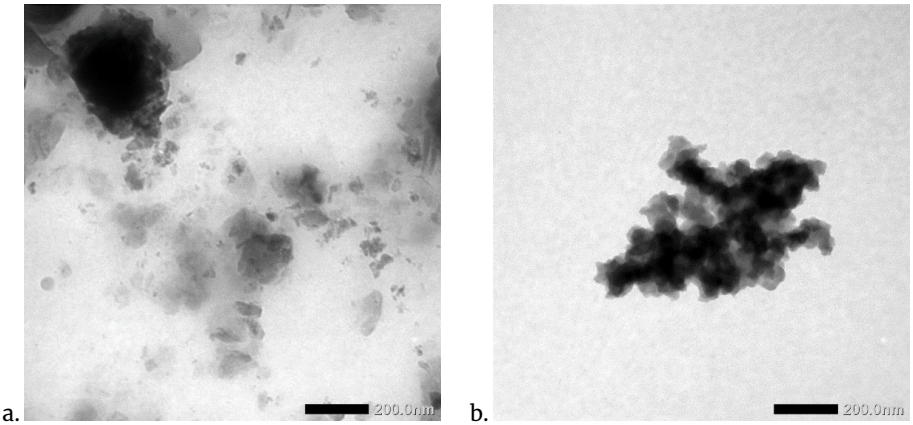

Figure 4. The images of Transmission Electron Microscopy (TEM) on (a) citric dispersed-activated iron sand and (b) (PB@SiO_2@TA)

TEM images of citric dispersed-activated iron sand and PB@SiO_2@TA at a magnification of 200 nm are shown in Figure 4.

From Figure 4a, it is observed that there are many gray parts, which are the layers of citrate and silica impurities in iron sand. Whereas in Figure 4b, PB@SiO_2@TA has a gray portion derived from a modified silica layer of the propyldiethylenetriammine group and has a black part, which is a magnetite oxide in iron sand. In the modified silica coating of the propyldiethylenetriammine group, citric dispersed-activated iron sand was added with 1 M HCl, which causes the citrate to release; hence the magnetite produces a Fe-OH group which allows reacting with the propyldiethylenetriammine modified silica. The acidified iron sand exchanges ligands with silica compounds, then the silica-based ligands undergo condensation and coat the surface of the magnetite, as stated by Hong *et al.* [22] and Susanto and Prasdiantika [30].

4. Conclusions

The results of XRF, FTIR, XRD, and TEM characterization showed that the iron sand in the Muara Kencan Beach, at Kendal Regency had a high iron oxide

content (81.66%) with a type of magnetic material was magnetite. The results of FTIR, XRD, and TEM characterization also showed that the iron sand hybrid nanomaterial coated with propyl diethylene triamine modified silica (PB@SiO_2@TA) was successfully synthesized with a crystal size of 36.21 nm and better particle dispersion compared to the prepared iron sand.

Acknowledgment

The author would like to thank the Directorate of Research and Community Service (DRPM) Kemenristekdikti, who has funded this research with the scheme of Hibah Penelitian Dosen Pemula in the 2019 budget year hence this research can be carried out well.

References

[1] Irina Ursachi, Aurelia Vasile, Horia Chiriac, Petronel Postolache, Alexandru Stancu, 2011, Magnetic properties of magnetite nanoparticles coated with mesoporous silica by sonochemical method, *Materials Research Bulletin*, 46, 12, 2468-2473 https://doi.org/10.1016/j.materresbull.2011.08.033

[2] Ibtisam Kamal, 2018, Prospects of Some Applications of Engineered Nanomaterials: A review, *Open Access Journal of Biomedical Engineering and Biosciences (OAJBEB)*, 2, 5, 149 http://dx.doi.org/10.32474/OAJBEB.2018.02.000149

[3] Vatara Artanta Silalahi, Enny Fachriyah, Pratama Jujur Wibawa, 2018, Isolation of Alkaloid Compounds from Ethanol Extract of Rimpang Galang Merah (Alpinia purpurata (Vielli) K. Schum) and nanoparticle production from its Alkaloid Extract. Comparative Study of Antibacterial Properties on Staphylococcus aureus and Eschericia, *Jurnal Kimia Sains dan Aplikasi*, 21, 1, 1-7 https://doi.org/10.14710/jksa.21.1.1-7

[4] Enny Fachriyah, Dewi Kusrini, Pratama Jujur Wibawa, 2018, Improvement of Bioactivity with Nanoparticle Fabrication: Cytotoxic Test of Ethanol, n-Hexane and Ethyl Acetate Extract from Red Galangal Rhizome (*Alpinia purpurata* (Vieill.) K. Schum) in Bulk and Nanoparticle Size using BSLT Method, *Jurnal Kimia Sains dan Aplikasi*, 21, 1, 39-43 https://doi.org/10.14710/jksa.21.1.39-43

[5] Emil Zacky Effendi, Yudhi Christian Hariady, Muhammad Daffa Salaahuddin, Chairul Irawan, Iryanti Fatyasari Nata, 2019, Utilization of Rice Husk Cellulose as a Magnetic Nanoparticle Biocomposite Fiber Source for the Absorption of Manganese (Mn^{2+}) Ions in Peat Water, *Jurnal Kimia Sains dan Aplikasi*, 22, 6, 220-226 https://doi.org/10.14710/jksa.22.6.220-226

[6] Gusti Ayu Dewi Lestari, Iryanti Eka Suprihatin, James Sibarani, 2019, Synthesis of Silver Nanoparticles (NPAg) using Andaliman (Zanthoxylum acanthopodium DC.) Fruit Water Extract and Its Application in Indigosol Blue Photodegradation, *Jurnal Kimia Sains dan Aplikasi*, 22, 5, 200-205 https://doi.org/10.14710/jksa.22.5.200-205

[7] Xiaolei Qu, Pedro J. J. Alvarez, Qilin Li, 2013, Applications of nanotechnology in water and wastewater treatment, *Water Research*, 47, 12, 3931-3946 https://doi.org/10.1016/j.watres.2012.09.058

[8] Yuanyuan Zhang, Qiang Xu, Shengxiao Zhang, Junshen Liu, Jing Zhou, Hui Xu, Huaqing Xiao, Jing Li, 2013, Preparation of thiol-modified Fe_3O_4@SiO_2 nanoparticles and their application for gold recovery from dilute solution, *Separation and Purification Technology*, 116, 391-397 https://doi.org/10.1016/j.seppur.2013.06.018

[9] Rochelle M. Cornell, Udo Schwertmann, 2006, *The Iron Oxides: Structure, Properties, Reactions, Occurrences and Uses*, 2nd ed., Wiley

[10] Dinas ESDM Jawa Tengah, 2018, *Peta Lokasi Pasir Besi Jawa Tengah*, Dinas ESDM Jawa Tengah, Semarang

[11] M. Helmi Rashid Farimani, N. Shahtahmasebi, M. Rezaee Roknabadi, N. Ghows, A. Kazemi, 2013, Study of structural and magnetic properties of superparamagnetic Fe_3O_4/SiO_2 core–shell nanocomposites synthesized with hydrophilic citrate-modified Fe_3O_4 seeds via a sol–gel approach, *Physica E: Low-dimensional Systems and Nanostructures*, 53, 207-216 https://doi.org/10.1016/j.physe.2013.04.032

[12] Wei Wu, Quanguo He, Changzhong Jiang, 2008, Magnetic Iron Oxide Nanoparticles: Synthesis and Surface Functionalization Strategies, *Nanoscale Research Letters*, 3, 11, 397 https://doi.org/10.1007/s11671-008-9174-9

[13] Wei Liu, Ping Yin, Xiguang Liu, Xiaoqi Dong, Jiang Zhang, Qiang Xu, 2013, Thermodynamics, kinetics, and isotherms studies for gold(III) adsorption using silica functionalized by diethylenetriamine methylenephosphonic acid, *Chemical Engineering Research and Design*, 91, 12, 2748-2758 https://doi.org/10.1016/j.cherd.2013.05.003

[14] Jiahong Wang, Shourong Zheng, Yun Shao, Jingliang Liu, Zhaoyi Xu, Dongqiang Zhu, 2010, Amino-functionalized Fe_3O_4@SiO_2 core–shell magnetic nanomaterial as a novel adsorbent for aqueous heavy metals removal, *Journal of Colloid and Interface Science*, 349, 1, 293-299 https://doi.org/10.1016/j.jcis.2010.05.010

[15] Xiao-Shui Li, Gang-Tian Zhu, Yan-Bo Luo, Bi-Feng Yuan, Yu-Qi Feng, 2013, Synthesis and applications of functionalized magnetic materials in sample preparation, *TrAC Trends in Analytical Chemistry*, 45, 233-247 https://doi.org/10.1016/j.trac.2012.10.015

[16] Nuryono Nuryono, Nur Mutia Rosiati, Bambang Rusdiarso, Satya Candra Wibawa Sakti, Shunitz Tanaka, 2014, Coating of magnetite with mercapto modified rice hull ash silica in a one-pot process, *SpringerPlus*, 3, 1, 515 https://doi.org/10.1186/2193-1801-3-515

[17] Hossein Mohammad-Beigi, Soheila Yaghmaei, Reza Roostaazad, Ayyoob Arpanaei, 2013, Comparison of different strategies for the assembly of gold colloids onto Fe_3O_4@SiO_2 nanocomposite particles, *Physica E: Low-dimensional Systems and Nanostructures*, 49, 30-38 https://doi.org/10.1016/j.physe.2013.01.004

[18] Koon Fung Lam, Chi Mei Fong, King Lun Yeung, Gordon McKay, 2008, Selective adsorption of gold from complex mixtures using mesoporous adsorbents, *Chemical Engineering Journal*, 145, 2, 185-195 https://doi.org/10.1016/j.cej.2008.03.019

[19] Susanto Susanto, Ricka Prasdiantika, Theodor CM Bolle, 2018, Pengaruh Pelarut terhadap Dispersi Partikel Fe_3O_4@ Sitrat, *Jurnal Sains Materi Indonesia*,

17, 4, 153-159
https://doi.org/10.17146/jsmi.2016.17.4.4176

[20] Shen Wu, Aizhi Sun, Fuqiang Zhai, Jin Wang, Wenhuan Xu, Qian Zhang, Alex A. Volinsky, 2011, Fe_3O_4 magnetic nanoparticles synthesis from tailings by ultrasonic chemical co-precipitation, *Materials Letters*, 65, 12, 1882-1884 https://doi.org/10.1016/j.matlet.2011.03.065

[21] Chao Hui, Chengmin Shen, Tianzhong Yang, Lihong Bao, Jifa Tian, Hao Ding, Chen Li, H. J. Gao, 2008, Large-Scale Fe_3O_4 Nanoparticles Soluble in Water Synthesized by a Facile Method, *The Journal of Physical Chemistry C*, 112, 30, 11336-11339 https://doi.org/10.1021/jp801632p

[22] Ruo-Yu Hong, Jian-Hua Li, Shi-Zhong Zhang, Hong-Zhong Li, Ying Zheng, Jian-min Ding, Dong-Guang Wei, 2009, Preparation and characterization of silica-coated Fe_3O_4 nanoparticles used as precursor of ferrofluids, *Applied Surface Science*, 255, 6, 3485-3492 https://doi.org/10.1016/j.apsusc.2008.09.071

[23] Happy Tan, Jun Min Xue, Borys Shuter, Xu Li, John Wang, 2010, Synthesis of PEOlated Fe_3O_4@SiO_2 Nanoparticles via Bioinspired Silification for Magnetic Resonance Imaging, *Advanced Functional Materials*, 20, 5, 722-731 https://doi.org/10.1002/adfm.200901820

[24] Eka Muliaty, 2014, Pelapisan Magnetit dengan Hibrida Merkapto-Silika untuk Adsorpsi Selektif Au (III) dari Sistem Multilogam Au (III)/Cu (II)/Ni (II), Departemen Kimia, Universitas Gadjah Mada, Yogyakarta

[25] M. E. Khosroshahi, L. Ghazanfari, 2010, Preparation and characterization of silica-coated iron-oxide bionanoparticles under N_2 gas, *Physica E: Low-dimensional Systems and Nanostructures*, 42, 6, 1824-1829 https://doi.org/10.1016/j.physe.2010.01.042

[26] C. Y. Haw, C. H. Chia, S. Zakaria, F. Mohamed, S. Radiman, C. H. Teh, P. S. Khiew, W. S. Chiu, N. M. Huang, 2011, Morphological studies of randomized dispersion magnetite nanoclusters coated with silica, *Ceramics International*, 37, 2, 451-464 https://doi.org/10.1016/j.ceramint.2010.09.010

[27] Ricka Prasdiantika, Susanto Susanto, 2017, Preparasi dan Penentuan Jenis Oksida Besi pada Material Magnetik Pasir Besi Lansilowo, *Jurnal Teknosains*, 6, 1, 7-15 https://doi.org/10.22146/teknosains.11385

[28] Susanto Susanto, Ricka Prasdiantika, Theodor C. M. Bolle, 2017, Sintesis Nanomaterial Magnetit-Sitrat dan Pengujian Aplikasinya sebagai Adsorben Emas (III), *Jurnal Teknosains*, 6, 2, 124-129 https://doi.org/10.22146/teknosains.10821

[29] Ricka Prasdiantika, Susanto Susanto, 2017, Preparasi Magnetit Pasir Besi Terdispersi Natrium Sitrat untuk Adsorpsi Au(III), *Neo Teknika*, 2, 2, 13-20

[30] Susanto Susanto, Ricka Prasdiantika, 2019, Pengaruh Rute Sintesis terhadap Keefektifan Pengikatan Gugus PDETA pada Sintesis Fe_3O_4@SiO_2@PDETA, *Jurnal Teknosains*, 8, 1, 39-47 https://doi.org/10.22146/teknosains.36264